# 2ND ORDER SPHERICAL HARMONIC SPATIAL ENCODING OF DIGITAL WAVEGUIDE MESH ROOM ACOUSTIC MODELS

*Alex Southern*

Audio Lab - Intelligent Systems Group
Department of Electronics
University of York
York, UK
YO10 5DD
aps502@ohm.york.ac.uk

*Damian Murphy*

Audio Lab - Intelligent Systems Group
Department of Electronics
University of York
York, UK
YO10 5DD
dtm3@ohm.york.ac.uk

**ABSTRACT**

The aim of this research is to provide a solution for listening to the acoustics of Digital Waveguide Mesh (DWM) modelled virtual acoustic spaces. The DWM is a numerical simulation technique that has shown to be appropriate for modelling the propogation of sound through air. Recent work has explored methods for spatially capturing a soundfield within a virtual acoustic space using spatially distributed receivers based on sound intensity probe theory. This technique is now extended to facilitate spatial encoding using second-order spherical harmonics. This is achieved through an array of pressure sensitive receivers arranged around a central reference point, with appropriate processing applied to obtain the second-order harmonic signals associated with Ambisonic encoding/decoding. The processed signals are tested using novel techniques in order to objectively assess their integrity for reproducing a faithful impression of the virtual soundfield over a multi-channel sound system.

## 1. INTRODUCTION

By providing a solution for the auralization of physically modelled enclosed acoustic spaces, this research aims to provide a means of synthesising both spatially and psychoacoustically realistic room impulse responses (RIR). In the longer term the Digital Waveguide Mesh (DWM) modelled RIR's may help measure some of the well documented limits of the DWM and provide information about any resulting psychoacoustical artefacts. Other common approaches of room acoustics modelling include the image-source method [1] and ray-tracing as used by ODEON [2] and pyramid tracing as in RAMSETE [3]. This research particularly focuses on providing spatial auralization of the modelled acoustic space, ideally in a manner that reproduces a pyschoacoustically faithful soundfield at the listener's ears. Previous work has explored the capture and decoding of a DWM simulated virtual 2D soundfield [4]. An orthogonal arrangement of 5 omni-directional receivers (7 for 3D), called a crux of receivers, has been shown to be a suitable technique for capturing a first-order B-Format Room Impulse Response (RIR) in a DWM. This paper proposes to extend this method by encoding the DWM synthesised soundfield to audio channels corresponding to the second-order channels associated with the Ambisonic multi-channel system.

The remainder of this paper is arranged as follows. In section 2 the digital waveguide is introduced and its role discussed in forming a DWM used to spatially measure RIRs. Section 3 reviews Ambisonics and B-Format theory, both briefly in terms of the encoding and decoding/rendering stage. In section 4 there is a review of previous techniques and results followed by an explanation of the proposed encoding techniques to be applied to the DWM model. Section 5 details the various testing techniques used to assess the success of the process from different perspectives, with results presented and analysed in section 6. Finally section 7 concludes the paper and suggests future points for consideration.

## 2. THE DIGITAL WAVEGUIDE

Digital waveguide synthesis was first introduced by J.O. Smith as a 1D computational physical modelling technique which found application in musical instrument synthesis, speech synthesis and acoustics [5]. Briefly the theory states that a travelling wave through a 1D system may be considered as the summation of two waves travelling in opposite directions. Mathematically this is expressed using d'Alembert's solution to the 1D wave equation which may be used to model a tube or vibrating string.

$$y(t,x) = y_r\left(t - \frac{x}{c}\right) + y_l\left(t + \frac{x}{c}\right) \quad (1)$$

Where $c$ is the speed of sound, $t$ is the current point in time (seconds), $x$ is the position along the string (metres) and $y_r$ & $y_l$ are the right and left going waves. The digital waveguide is a discrete implementation of (1) that in practice is represented using a bi-directional digital delay line as shown in Figure 1.

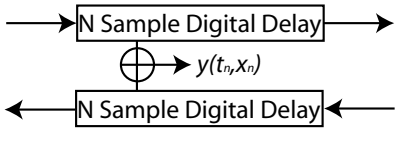


Figure 1: *The bi-directional digital delay line that forms the basic 1D digital waveguide.*

The discrete time implementation of (1) is given by (2) which mathematically expresses the use of the bi-drectional delay lines in Figure 1 forming the basic digital waveguide [6].

$$y(t_n, x_m) = y^+(n-m) + y^-(n+m) \quad (2)$$

Where $y(t_n, x_m)$ is the physical amplitude output at time sample $t_n$ at position $x_m$ along the bi-directional delay line and $n = nT$ and $m = mT$ when $T$ is sampling interval in seconds. $y^+$ and $y^-$ are digital equivalent of the continuous time domain signals $y_r$ and $y_l$.

### 2.1. The Digital Waveguide Mesh

The DWM is comprised of multiple digital waveguides which may extend the system to 2D, 3D or higher dimensions. The extension of the digital waveguide to the 2D case has previously been discussed as a means of modelling membranes, e.g. [7]. In Figure 2 it may be observed that the nodes are connected by the same bi-directional delay lines shown in Figure 1. The delay between each node is 1 sample and it has been shown that these systems are capable of modelling a range of resonant objects with different degrees of dimensionality [8].

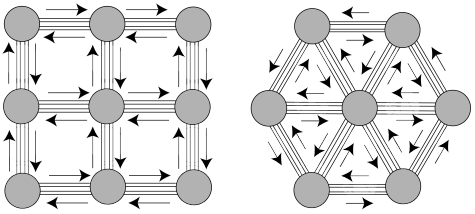

Figure 2: *The rectilinear and triangular DWM topologies*

This work has been conducted using a research tool called *RoomWeaver* which is a result of previous work at the University of York [9]. This software may be used to design virtual geometric representations of acoustic environments and then properly calculate the associated RIR. Recent work has shown how to synthesise B-Format RIRs from the DWM model in *RoomWeaver* [4] [10].

## 3. AMBISONICS ENCODING AND DECODING

Ambisonics describes a method of capturing/encoding a 3D soundfield by means of its spherical harmonic decompostion to the $n^{th}$ order around a spatial reference point [11]. These signals may then be decoded to a loudspeaker arrangment, although the exact decoding equations will change primarily depending on the loudspeaker positions and many decoding schemes have been discussed previously e.g. [12] [13] [14]. Figure 3 shows the 3D polar responses associated with each channel of a 2nd order system. W is an omnidirectional pressure signal, and XYZ correspond to 3 velocity signals arranged orthogonally along the cartesian axes. Collectively these 1st order system signals WXYZ are known as B-Format. A full 2nd order system consists of the 1st order WXYZ channels and the channels RSTUV. The polar responses shown in Figure 3 are described in (3) using the appropriate corresponding ambisonic encoding equations [15].

$$
\begin{aligned}
W &= 0.707107 \\
X &= \cos(\theta_A) \cdot \cos(\theta_E) \\
Y &= \sin(\theta_A) \cdot \cos(\theta_E) \\
Z &= \sin(\theta_E) \\
R &= 1.5 \sin^2(\theta_E) - 0.5 \\
S &= \cos(\theta_A) \cdot \sin(2\theta_E) \\
T &= \sin(\theta_A) \cdot \sin(2\theta_E) \\
U &= \cos(2\theta_A) \cdot \cos^2(\theta_E) \\
V &= \sin(2\theta_A) \cdot \cos^2(\theta_E)
\end{aligned} \tag{3}
$$

Where $\theta_A$ and $\theta_E$ are the sound source azimuth and elevation respectively. Note that it is also possible to consider ambisonics for the horizontal plane only. In this case all expressions containing $\theta_E$ may be omitted as they all become equal to one when $\theta_E = 0$. Therefore the horizontal 1st order case only requires WXY channels. WXYUV channels are required for 2nd order horizontal ambisonics and therefore these are the channels that will be encoded from the DWM in this work.

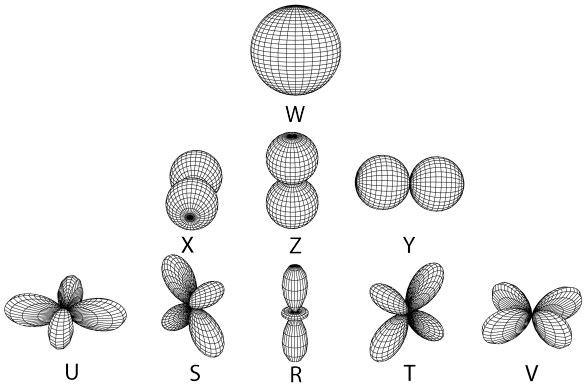


Figure 3: *Spherical harmonics upto 2nd order*

## 4. ENCODING TECHNIQUES

Two different approaches for encoding the DWM into B-Format have been considered previously. The first consisted of a circle of receivers with the second using an arrangement based on a crux of receivers, both of which are shown in Figure 4. Receivers are defined as pressure sensors that form the fundamental sampling method in the DWM. In [10] it was shown that the circle of receivers method does not perform reliably, primarily due to fact that it does not discrimate between wavefronts entering and leaving the circle.

Only the crux method will be considered here as this research focuses on extending the current technique to capture the 2nd order spherical harmonics. However a more comprehensive measurement method using a circle of 1st order receivers has been presented previously for real rooms in [16].

Figure 4: *The circle and 2D crux of receivers*

### 4.1. Capturing 1st Order Components

Previous work has shown that the 1st order spherical harmonics or B-Format signal may be obtained from the DWM [4] [10]. The fundamental technique on which this is based is a process more commonly associated with p-p sound intensity probes for the calculation of velocity at a point. Equation 4 expresses the velocity component in terms of two closely spaced pressure sensors [17].

$$u(t) \approx \left(\frac{1}{\rho_0 \cdot d}\right) \int_0^{\infty} [p_1(t) - p_2(t)]\, \delta t \tag{4}$$

Where $\rho_0$ is the density of air, $d$ is the distance between pressure sensors and $p_1(t)$ and $p_2(t)$ are the pressure at time $t$ at each sensor. For a more detailed account of using this technique for capturing the X and Y velocity components see [10]. However we will briefly include a preliminary study in order to demonstrate this technique with a view to extending the test to the 2nd order case. The test involves placing two closely spaced receivers into a simulated acoustic free field and then rotating the position of an impulse sound source at a fixed radius of 1 metre every 22.5°. Figure 5(a) illustrates the setup for the test. At each source position the two receivers are processed appropriately according to (4) and the sample value of the main peak is plotted against its angle with the results shown in Figure 5(b).

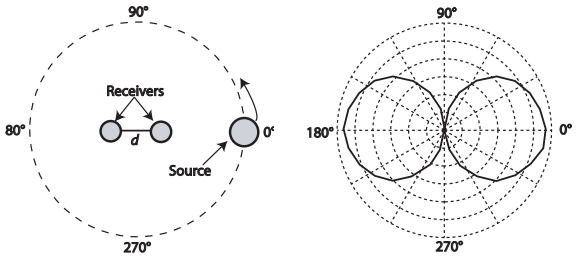


Figure 5: *Preliminary test for capturing ambisonic velocity components*

Therefore Figure 5(b) clearly illustrates that (4) provides directional discrimination which results in the corresponding velocity pattern.

### 4.2. Capturing 2nd Order Components

Horizontal 2nd order ambisonics comprises signals WXYUV. The method for obtaining X and Y has been described above, while W is simply captured by placing a receiver at the central reference position. The U and V channels are therefore required to complete the signal, a method is proposed in the following.

Prior to this paper, the TKK microphone arrangement has been shown to be capable of forming highly directional beams from a spaced array of omnidirectional capsules [18]. The microphone is described as being suitable for capturing 1st order B-Format signals [19]. For capturing 2nd order components it is presented that the microphone array is able to form the associated polar pickup patterns but for a reduced frequency band [18] [19]. More generally the process of using lower order microphone capsules to provide higher order directional responses has been termed the *Blumlein Difference Technique* and various cases are discussed in [20] [21].

Equations (5) and (6) describe U and V respectively in terms of the X and Y signals according to [18].

$$U = X^2 - Y^2 \tag{5}$$

$$V = X \cdot Y \tag{6}$$

Therefore in order to obtain the X and Y velocity components the arrangment of receivers shown in Figure 6(a) is used. Capturing the 1st order pressure gradient from two pressure sensors was discussed in section 4.1, while capturing the 2nd order pressure gradient may be achieved from (5) and (6).

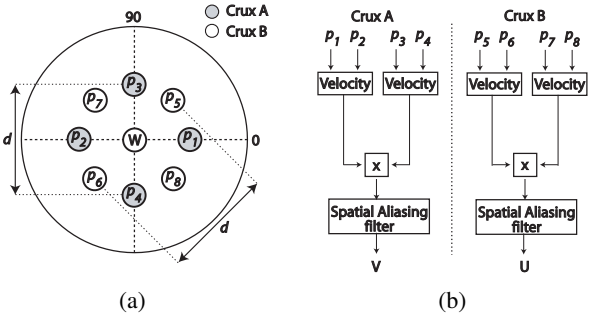


Figure 6: *Proposed arrangment of receivers for 2nd order encoding along with a basic encoding strategy*

Figures 6(a) & (b) break down the calculation of the UV channels from the 4 receivers labelled Crux A and Crux B. An alternative yet similar approach for processing the 2nd order components may be employed by extending the technique presented in [20] to obtain the receiver arrangement in Figure 6(a). Another preliminary test is presented which aims to initially verify the worth of the proposed 2nd order encoding technique. The test is carried out in the same manner as shown in Figure 5(a) however the difference being that the four receivers labeled Crux B are used as arranged in Figure 6(a). The processing carried out is used to obtain the polar pattern associated with the U channel, which is given in (3) and plotted in Figure 7(a). Figure 7(b) is the resulting polar pickup pattern of the array in Figure 6 after processing. For clarity Figure 7(c) is provided so that a direct comparison of the desired theoretical response and actual response can be made after normalising the amplitude values. Equations (5) & (6) may describe how to obtain the UV channels from using Crux A, however (5) requires two multiplies with the associated potential for a loss of accuracy, hence resulting in greater numerical error. Consequently Crux B is used to minimize this effect.

This preliminary test has confirmed that it is possible to obtain the necessary gain response for the U channel using the X and Y velocity signals. However the test tells us nothing about the directionally dependent frequency response or the reliability of this technique for facilitating higher resolution spatial rendering of virtual acoustic spaces.

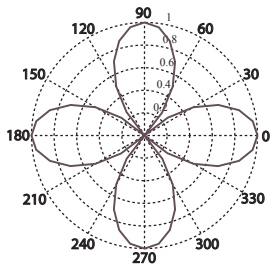


(a) Theoretical Response

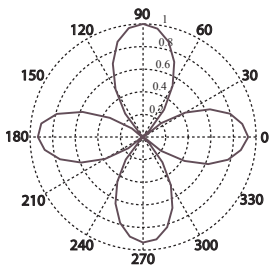


(b) Preliminary test response

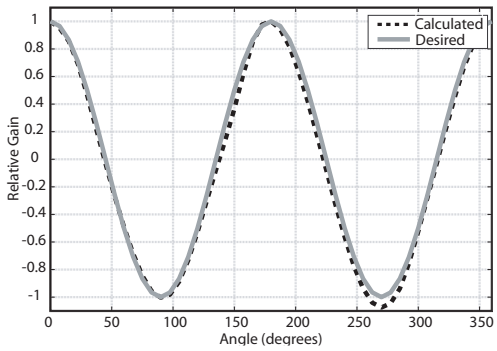


(c) Theoretical and test responses superimposed

Figure 7: *Preliminary test results for 2nd order encoding*

## 5. TESTING TECHNIQUES

Numerous testing strategies are employed for evaluating the performance of the 2nd order channels and are as follows:

- AmbiMeter (Polar Plot)
- AmbiMeter (Time Vs. Angle of Arrival)
- Directionally dependent frequency response analysis

### 5.1. The *AmbiMeter* Measures

The *AmbiMeter* measures were previously presented for 1st order signal evaluation in [10]. The term *AmbiMeter* decribes the name given to a specifically designed software application used for generating the resultant polar plots. For this work, in each case, the input signal must be a 2nd order B-Format RIR. The polar plot may only be used to assess the direct sound portion of the RIR while the Time Versus Angle (TVA) plot has been shown to be appropriate for inspecting the arrival of early reflections. The software operates by ambisonically decoding the signal to 144 equally spaced virtual loudspeaker directions on a circle using (7).

$$S_i = 0.5 \cdot ((2-d) \cdot W \cdot 1.4142) + d \cdot (\cos\theta_i \cdot X + \sin\theta_i \cdot Y + \cos 2\theta_i \cdot U + \sin 2\theta_i \cdot V) \quad (7)$$

Where $S_i$ is the $i^{th}$ speaker, $\theta_i$ is the angular position of that speaker and $d$ is a directivity factor, varying between 0 and 1, as discussed in [12] [13]. The amplitude of the loudspeaker signals is then plotted and used to identify the direction from which the direct and early reflected sounds will arrive. For the polar plots the ampltude of the direct sound peak is plotted against the loudspeaker signal azimuth whereas in the TVA plots the amplitude at each time sample and loudspeaker angle is indicated using the gray scale plot. The results of the TVA plots are confirmed by using the ray tracing technique to accurately estimate the time and angle of arrival of wavefronts. Figure 8 illustrates the setup of the TVA tests and the associated early reflection predictions.

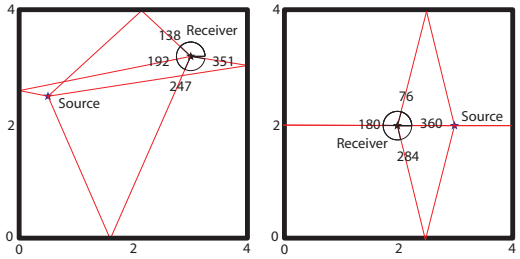


Figure 8: *Scaled images of the TVA test setup and resulting rays*

A 4m by 4m room and a 2D DWM are used to model the propogation of sound on the horizontal plane. Table 1 provides the estimated time and angle of arrival of the 1st order reflections labelled R1 to R4 in chronological order when the source and receiver is placed respectively at [0.5,2.5] and [3,3.2] for TVA test 1 and at [3,2] and [2,2] for TVA test 2. This is used as a measure for assessing that the receiver array encoding scheme in Figure 6 is correctly capturing the DWM modelled soundfield to the 2nd order. This is acheived by comparing the actual wavefront time and angle of arrival to the estimated one.

| Test 1 | D | R1 | R2 | R3 | R4 |
|---|---|---|---|---|---|
| Angle | 196 | 137 | 191 | 350 | 246 |
| Time(s) | 0.0076 | 0.0099 | 0.0104 | 0.0133 | 0.0183 |
| Test 2 | | | | | |
| Angle | 0/360 | 0/360 | 76 | 284 | 180 |
| Time(s) | 0.0029 | 0.0088 | 0.0121 | 0.0121 | 0.0147 |

Table 1: *Estimated times and angles of arrival of the first four reflections in Tests 1 and 2*

### 5.2. The Directionally Dependent Frequency Response

Directionally dependant frequency response analysis is used to assess how well the encoding technique matches the theoretical/ideal polar response as shown in Figure 7(a) for specific frequencies. The source signal is moved around the array of receivers at a constant distance and the U and V channels are calculated according to Figure 6(b). For a specific frequency the magnitude is plotted against the angle of the impulse sound source to provide a frequency dependent polar plot.

## 6. RESULTS ANALYSIS

The results for the *AmbiMeter* polar plot tests are presented in Figure 9. The 2nd order lobes point towards the direction of the sound

source which was placed at $0°, 90°, 180°$ and $270°$ in (a) and at $45°, 135°, 225°$ and $315°$ in (b) at 1 metre. This suggests that if the 2nd order B-Format signal was decoded to an appropriate loudspeaker array rather than a polar plot, the direct sound would be loudest at the desired angle.

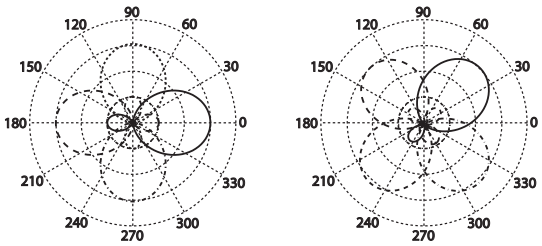


Figure 9: *AmbiMeter polar plot results for a sound source at 1m every* $45°$

In Figure 10 the results are presented for the first TVA test. The estimated time and angle of arrival for direct and reflected wavefronts are denoted by D and R1-R4. It may be observed that there are other reflections that are not predicted by the ray tracing technique in Table 1. Some of these occur before all of the 1st order reflections have arrived. Table 1 only estimates the 1st order reflections and these will not necessarily be the first four reflections to arrive at the microphone position. Therefore the other unlabelled wavefronts are 2nd order reflections and above, this will be demonstrated using Figure 11.

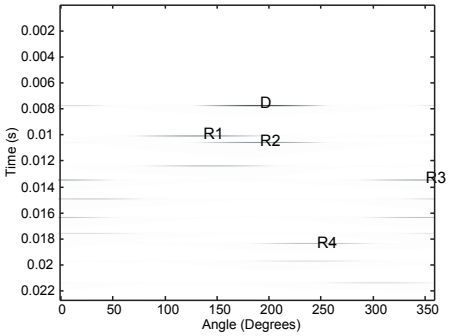


Figure 10: *Result for the first Time vs Angle AmbiMeter test*

Figure 11 is the second *AmbiMeter* TVA test result and in this case no 2nd order reflections arrive before R2 and R3. However R4 appears to arrive from all directions rather than $180°$. This is due to the fact that two other 2nd order reflections arrive at approximately the same time from different angles. This demonstrates how 2nd order reflections can seemingly obscure the estimated 1st order reflections. For clarity the time and angle of arrival values for the two suspected 2nd order reflections are calculated. Figure 12 illustrates the suspected movement of the 2nd order wavefronts. It is possible to easily evaluate the boundary location co-ordinates B1 - B2 for R5 and R6 in this simple room, and these are provided in Table 2.
As the source and receiver positions are also known it is possible to use simple trigonometry to calculate the path length and angle of arrival for reflections 5 and 6. These are also presented in Table 2 and are placed onto the TVA test axis for completeness in Figure 13. In both cases it is clear that the predicted reflections arrive at the microphone position at the estimated time and angle of arrival.

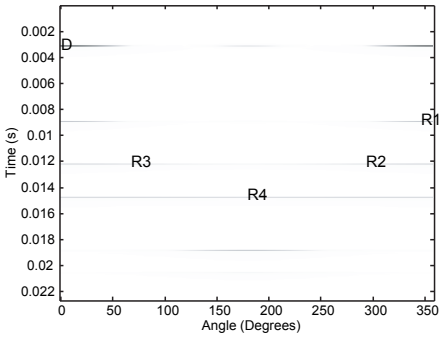


Figure 11: *Result for the second Time vs Angle AmbiMeter test*

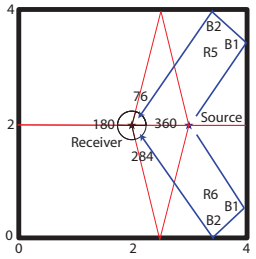


Figure 12: *Illustration of the path of two 2nd order reflections*

| | Dist(m) | Arrival Time(s) | Angle | B1 [x,y] | B2 [x,y] |
|---|---|---|---|---|---|
| R5 | 5.2 | 0.0155 | 53 | [4, 3.5] | [3.5, 4] |
| R6 | 5.2 | 0.0155 | 306 | [4, 0.5] | [3.5, 0] |

Table 2: *Path distance along with estimated time and angle of arrival for R5 and R6*

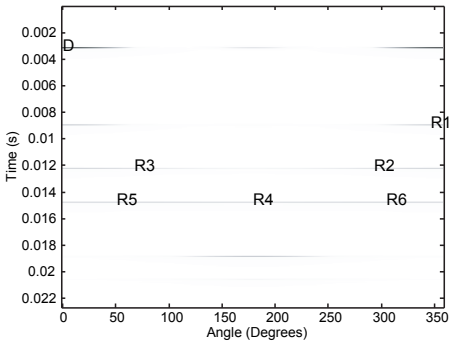


Figure 13: *Identification of the two 2nd order reflections*

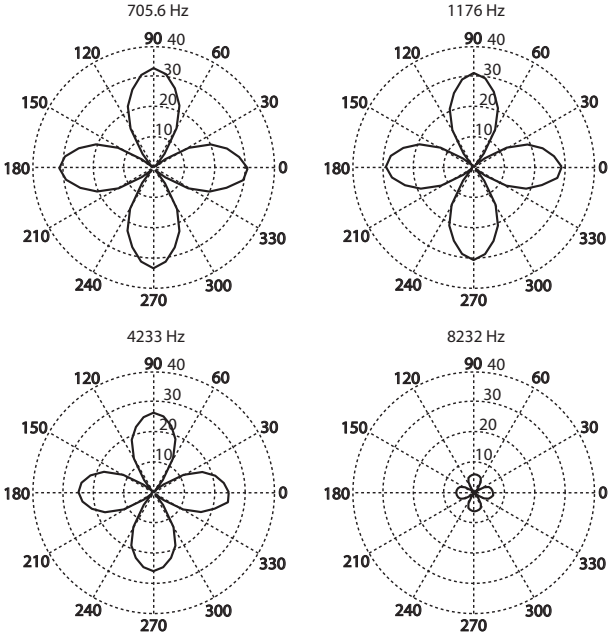


Figure 14: *U channel frequency dependent polar plots*

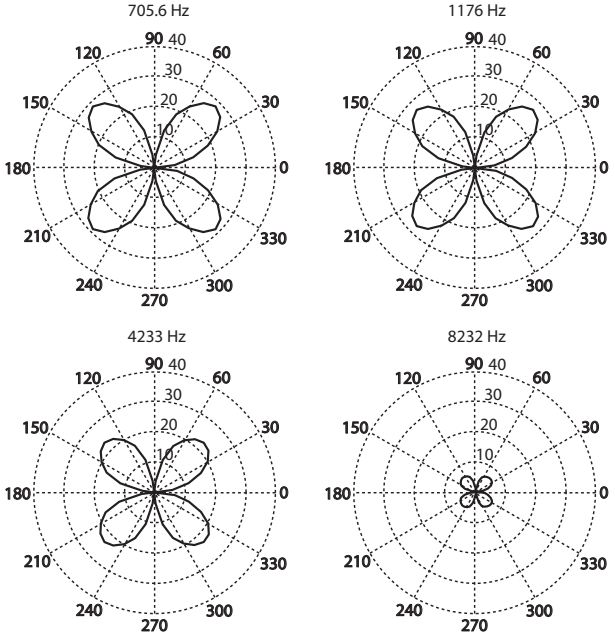


Figure 15: *V channel frequency dependent polar plots*

An indication of the actual sound pressure level is not necessary at this stage as the performance of the virtual microphone is not under test here. Rather the TVA tests help to provide a proof of concept in this work.

### 6.1. Directionally Dependent Frequency Response Results

The frequency dependent polar plots are presented for the both the U and V channels at four different frequencies chosen to sample the directional response across the usable range upto, but below, the spatial aliasing frequency. The spatial aliasing frequency is defined as the frequency whose wavelength is half the distance between the sampling points. Frequencies with smaller wavelengths are not supported and therefore must be filtered out in order to avoid ambiguity. The spatial aliasing frequency is defined in (8) as in [20] [22].

$$f_{sp} = \frac{c}{2 \cdot \Delta_{transducer}} \tag{8}$$

Where $f_{sp}$ is the spatial alisaing frequency in Hertz, $c$ is the speed of sound in air and $\Delta_{transducer}$ is the distance between the two pressure sensors/receivers in metres. For these tests a spacing of $d$ = 0.04m was used (see Figure 6(a)) and so from (8) $f_{sp}$ = 4.25kHz. The DWM model used a sampling frequency of 176.4kHz which corresponds to an internodal distance of 0.0027m. It should be noted that this sampling rate will support a smaller receiver spacing and hence a higher $f_{sp}$ than that chosen. However issues arise as receiver positions can only exist at node positions which may or may not be at the numerically exact spatial co-ordinates associated with the virtual microphone array.

Figure 14 presents the frequency dependent polar plots for the U channel with Figure 15 showing the V channel response. Note that the radial axis is in dBs however the scale is not logarithmic for convenience. Figures 14 & 15 both indicate that the encoding techniques are approximately directionaly discriminating the incoming wavefronts at the correct azimuths in order to produce the desired polar response described by U and V in (3). It may be observed that theoretically the polar patterns for U and V should be identical but with a 45° rotation. Comparing the actual response for any pair of frequencies reveals that while the 45° rotation holds, the actual polar responses are not identical. The cause of this is the same reason that a smaller receiver spacing has not been chosen, the DWM is a discrete representation of a continuous medium. For example, when positioning two receivers with a distance of 0.02m apart in the DWM it is almost certain that these will not be exactly 0.02m apart. This is because the receiver position is 'snapped' to the closest DWM node position resulting in the apparent discrepancy. With relation to the proposed receiver arrangement, it is reasonable to assume that Crux A and B will introduce differing amounts of this discrepancy as they are orientated differently in the DWM. Therefore this issue may be improved if the DWM sampling frequency increases to infinity, which ensures that the distance between adjacent DWM nodes becomes infinitely small or alternatively the sound pressure between DWM nodes is accurately interpolated.

It is also apparent that the results are not consistent across the frequency spectrum, even when considering the few cases presented above. In addition, it might also be concluded that the polar response pattern worsens as frequency increases which is expected as the frequency wavelength reaches twice the receiver spacing [20] [23]. The relative gains of the virtual microphone also decreases as frequency increases. This apparent decrease may be attributed to two factors. The first being that as the frequency under test approaches the spatial aliasing frequency the anti-spatial aliasing filter will begin to reduce the gain. Secondly low frequencies are boosted for closer sound sources according to the proximity effect which is accentuated more as microphone order increases [23] [24]. Nevertheless the results are very encouraging and suggest that the proposed technique is working, although with some reser-

vations as to its performance with respect to frequency response. It should be pointed out that similar effects will occur with real microphone arrays as their sensitivities will not be identical [20].

## 7. CONCLUSIONS

This paper has proposed an encoding technique for the capture of 2nd order spherical harmonics in the horizontal plane for virtual acoustic models based on the digital waveguide mesh. The results have indicated that this initial encoding process is capable of effectivley sampling the virtual soundfield, although at this point the frequency response is still not ideal. The directionally dependent frequency response in conjunction with the *AmbiMeter* tests suggest that the calculated UV channels are able to provide an end listener with the directional characteristics of a DWM modelled acoustic space based on spherical harmonics to 2nd order. The frequency dependent polar plots also indicate that post-capture calibration must be carried out in order smooth out the main operational frequency band and this will be addressed in future work.

## 8. ACKNOWLEDGMENTS

This work has been supported by the University of York, Department of Electronics, EPSRC Doctoral Training Grant.

## 9. REFERENCES

[1] J.B. Allen & A. Berkley, "Image method for efficiently simulating small-room acoustics," *J.Acoustic Society of America*, vol. 75, no. 4, pp. 943–950, 1979.

[2] ODEON A/S, "Odeon room acoustics software," Available at http://www.odeon.dk, Accessed March 21, 2007.

[3] A. Farina, "Ramsete: Room acoustics modeling on pc," Available at http://pcfarina.eng.unipr.it/ramsete_ultimo/index.htm, Accessed March 20, 2007.

[4] A. Southern & D. Murphy, "Spatial encoding for digital waveguide mesh room modeling applications," in *Proc. of the AES 28th International Conference: The future of surround and beyond, Piteå, Sweden*, July 2, 2006, pp. 188–91.

[5] J.O. Smith, "A new approach to digital reverberation using closed waveguide networks," in *Proc. of 1985 International Computer Music Conference, Vancouver, Canada*, 1985, pp. 47–53.

[6] J.O. Smith, "Physical modeling using digital waveguides," *Computer Music Journal*, vol. 16, no. 4, pp. 74–91, 1992.

[7] S.A. Van Duyne & J.O. Smith, "Physical modeling with the 2-d digital waveguide mesh," in *Proc. of Int. Computer Music Conf, Tokyo, Japan*, 1993, pp. 40–47.

[8] D.T. Murphy, A. Kelloniemi, J. Mullen, and S. Shelley, "Acoustic modeling using the digital waveguide mesh," *IEEE Signal Processing Magazine*, vol. 24, no. 2, pp. 55–66, 2007.

[9] M.J. Beeson and D.T. Murphy, "Roomweaver: A digital waveguide mesh based room acoustics tool," in *Proc. of 7th International Conference of Digital Audio Effects (DAFx-04), Naples, Italy*, 2004, pp. 268–273.

[10] A. Southern, "Spatial rendering of digital waveguide mesh room acoustic models for multichannel sound," M.S. thesis, Department of Electronics, The University of York, UK, 2006, Available at http://www-users.york.ac.uk/~aps502/pubs.html.

[11] M.A. Gerzon, "With-height sound reproduction," *Journal of the Audio Engineering Society*, vol. 21, pp. 2–10, 1973.

[12] A. Farina, R. Glasgal, E. Armelloni, and A. Torger, "Ambiophonic principles for the recording and reproduction of surround sound for music," in *Proc. of 19th AES Conference on Surround Sound Techniques, Technology and Perception, Schloss Elmau, Germany*, 2001, pp. 21–24.

[13] B.J. Wiggins, *An Investigation into the real-time manipulation and control of three-dimensional sound fields*, Ph.D. thesis, University of Derby, UK, 2004, Available at http://sparg.derby.ac.uk/SPARG/PDFs/BWPhDThesis.pdf.

[14] R. Furse, "First and second order ambisonic decoding equations," Available at http://www.muse.demon.co.uk/ref/speakers.html, Accessed March 21, 2007.

[15] D. Malham, "Second and third order ambisonics - the furse-malham set," Available at http://www.york.ac.uk/inst/mustech/3d_Audio/secondor.html, Accessed March 21, 2007.

[16] M.A. Poletti, "A unified theory of horizontal holographic sound systems," *Journal of the Audio Engineering Society*, vol. 48, no. 12, pp. 1155–1182, 2000.

[17] F.J. Fahy, *Sound Intensity*, Elsevier Applied Science, London, 1989.

[18] J. Merimaa, "Applications of a 3d microphone array," in *Audio Engineering Society 112th Convention, Munich, Germany*, 2002.

[19] J. Merimaa, *Analysis, Synthesis and Perception of spatial sound - Binaural Auditory modeling and multichannel loudspeaker reproduction*, Ph.D. thesis, Helsinki University of Technology, 2006, Available at http://lib.tkk.fi/Diss/2006/isbn9512282917/.

[20] M.A. Gerzon, "Ultra-directional microphones - part 1," *Studio Sound*, pp. 434–437, October, 1970.

[21] P.S. Cotterell, *On the Theory of the Second-Order Soundfield Microphone*, Ph.D. thesis, University of Reading, 2002, Available at http://www.ambisonic.net/pdf/CotterellThesis/.

[22] J. Daniel, R. Nicol, and S. Moreau, "Further investigations of high order ambisonics and wavefield synthesis for holophonic sound imaging," in *Proc. of 114th AES Convention*, 2003.

[23] M.A. Gerzon, "Ultra-directional microphones - part 2," *Studio Sound*, pp. 501–504, November, 1970.

[24] M.A. Gerzon, "Ultra-directional microphones - part 3," *Studio Sound*, pp. 539–543, December, 1970.